ROTATION SENSORS BASED ON ATOM INTERFEROMETRY

Christian Schubert, A. Wacker, M. Eichelmann, S. Gerlach, C. Deppner, H. Ahlers, W. Herr

Deutsches Zentrum für Luft- und Raumfahrt e. V. (DLR), Institut für Satellitengeodäsie und Inertialsensorik, Hannover, Germany

M. Gersemann, S. Abend, E. M. Rasel

Leibniz Unversität Hannover, Institut für Quantenoptik, Hannover, Germany

DLR

Motivation for atom interferometry rotation sensors

Applications in navigation, geodesy, fundamental physics

Providing absolute, long-term stable measurements

Complementary to established sensors (MEMS, ring laser gyros, fibre gyros, …)

Potential for miniaturisation – intermediate sized sensor with high performance

Atom interferometry

Absolute, stable measurements; atoms in free fall, Mach-Zehnder like π/2 – π – π/2 pulse geometry:

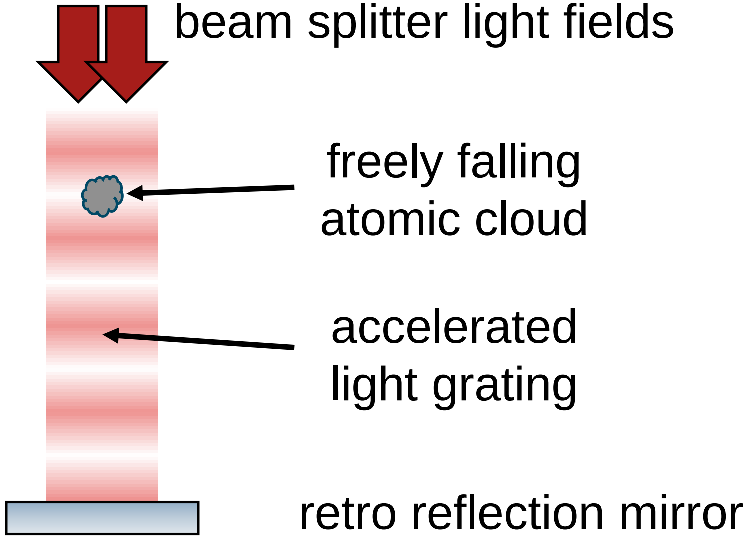

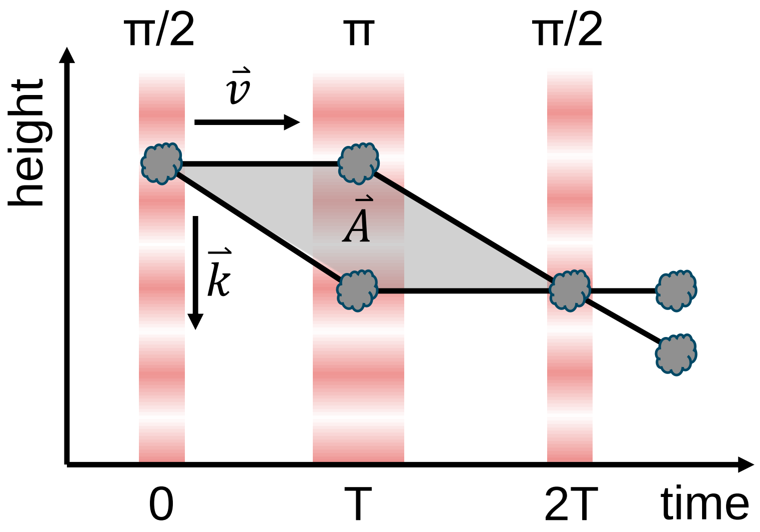

Interferometer phase, ϕ_i imprinted at pulse i: $\phi_{tot} = \phi_1 - 2\phi_2 + \phi_3$

Acceleration $\vec{a}$, effective wave vector $\vec{k}$: $\phi_{acc} = \vec{\boldsymbol{k}} \cdot \vec{a}\, \boldsymbol{T}^2$

Forward drift velocity $\vec{v}$, rotation $\vec{\Omega}$, enclosed area $\vec{A}$: $\phi_{rot} = 2\left(\vec{\boldsymbol{k}} \times \vec{v}\right) \cdot \vec{\Omega}\, \boldsymbol{T}^2 \sim \vec{\boldsymbol{A}} \cdot \vec{\Omega}$

Shot noise limit

3-pulse atom interferometer (AI), Mach-Zehnder like:

$$\sigma_{a,sn} = \frac{1}{C\sqrt{N}\cdot 2\cdot k\cdot v\cdot T^2}\sqrt{\frac{T_c}{\tau}}$$

C: contrast
N: number of atoms
k: effective wave number
v: drift velocity, $\mathrm{v} \perp k$
T: free evolution time
T_c: cycle time
τ: integration time

Colder atoms / low expansion rates → increased C, k, T

High flux sources → increased N, decreased T_c

→ **reduced shot noise**

4-pulse geometry

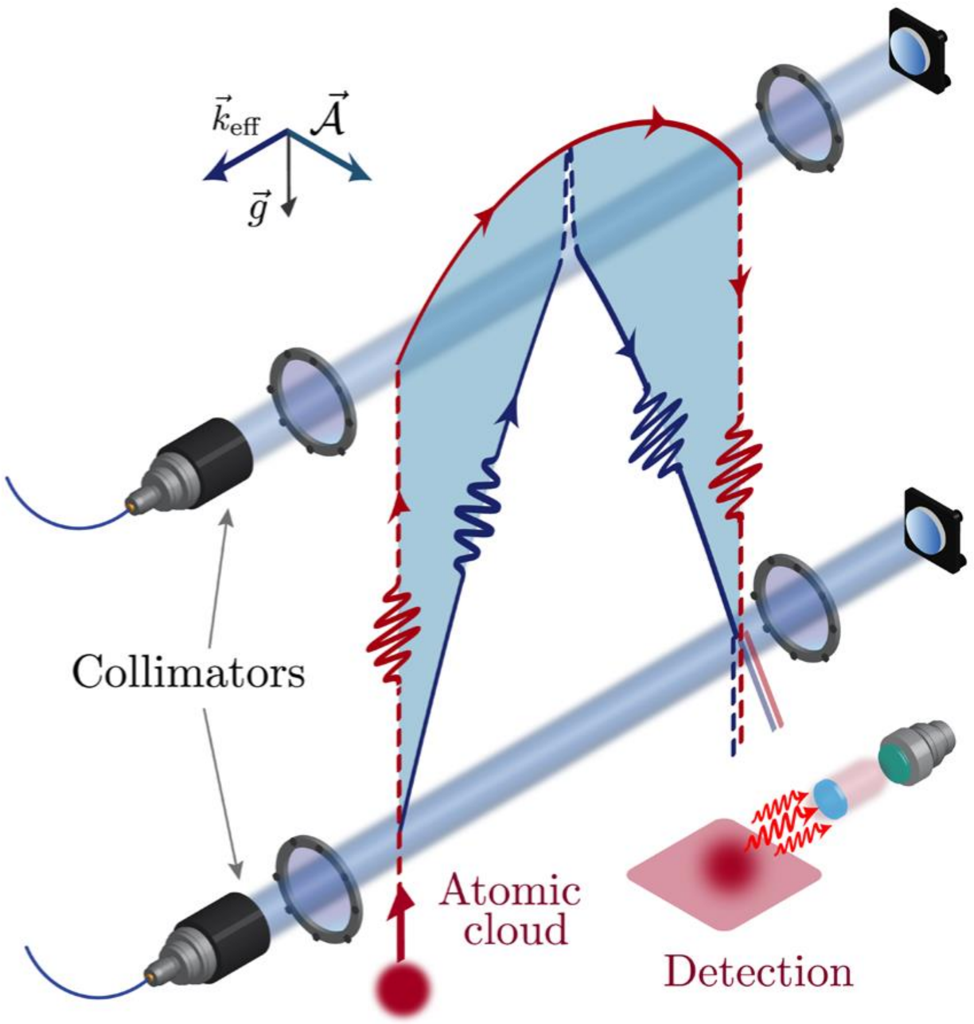

Image from [1]

Atoms in free fall, π/2 – π – π – π/2 pulse geometry

Free-fall time T, effective wave vector $\vec{k}$, gravitational acceleration $\vec{g}$, rotation $\vec{\Omega}$:

$$\phi_{rot} = \frac{T^3}{2}\left(\vec{k} \times \vec{g}\right) \cdot \vec{\Omega}$$

[Images and results from: 1) Gautier et al., Sci. Adv. 8, eabn8009 (2022), CC BY 4.0, https://creativecommons.org/licenses/by/4.0/; see also: Stockton et al., PRL 107, 133001 (2011); Canuel et al., PRL 97, 010402 (2006)]

State of the art in AI-based quantum sensors

Rotation sensors

Stability:
- 30 nrad/s in 1s
- 0.1 nrad/s after averaging

Uncertainty:
- Few nrad/s to 10 nrad/s

Gravimeters

Stability:
- 42 nm/s^2 in 1s
- 0.5 nm/s^2 after averaging

Systematic uncertainty:
- 40 nm/s^2
- Limited by wave front distortions 1)

Transportable, sea, flight, commercial versions

Gravity gradiometers

Stability:
- $3\cdot10^{-8}$ $1/s^2$ in 1s

Systematic uncertainty
- $8\cdot10^{-8}$ $1/s^2$

Determination of gravitational constant

[From: Chen et al., arXiv:2303.00239; Gautier et al., Sci. Adv. 8, eabn8009 (2022); Berg at al., PRL 114, 063002 (2015); Stockton et al., PRL 107, 133001 (2011); Gauguet et al., PRA 80, 063604 (2009); Gillot et al., Metrologia 51, L15-L17 (2014); 1) reduced in Karcher et al., NJP 20, 113041 (2018); Freier et al., JoP:CS 723, 012050 (2016); Hu et al., PRA88, 043610 (2013); Wu et al., Sci. Adv. 5, eaax0800 (2019); Bidel et al., Nat.Comm. 9, 2041 (2018); Bidel et al., JoG 94, 1432 (2020); muquans.com; McGuirk et al., PRA 65, 033608 (2002); Fixler et al., Science 315, 74 (2007); Biedermann et al., PRA 91, 033629 (2015); Chiow et al., PRA 93, PRA 93, 013602 (2016); Rosi et al., Nature 510, 518 (2014); Asenbaum et al. PRL 118, 183602 (2017)]

Cold atom Sagnac interferometer (CASI)

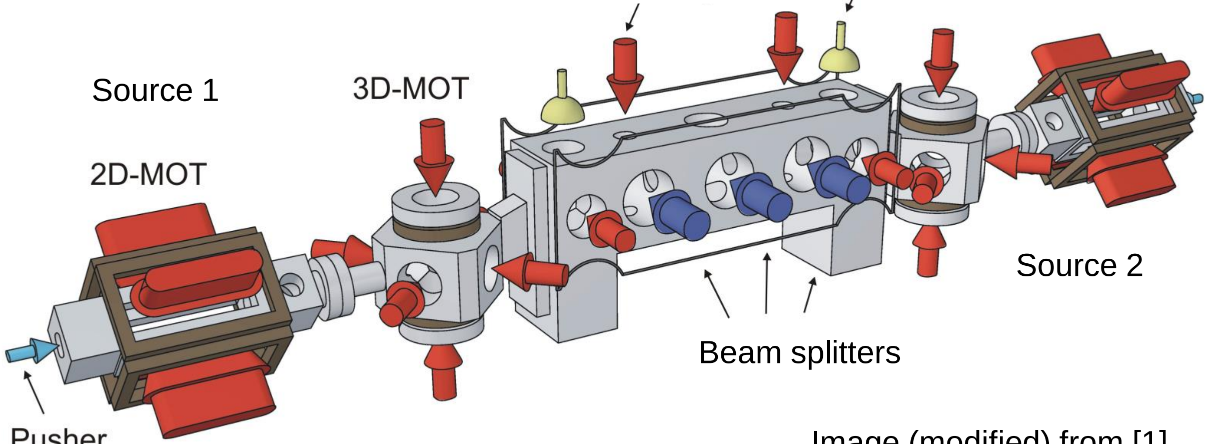

Image (modified) from [1]

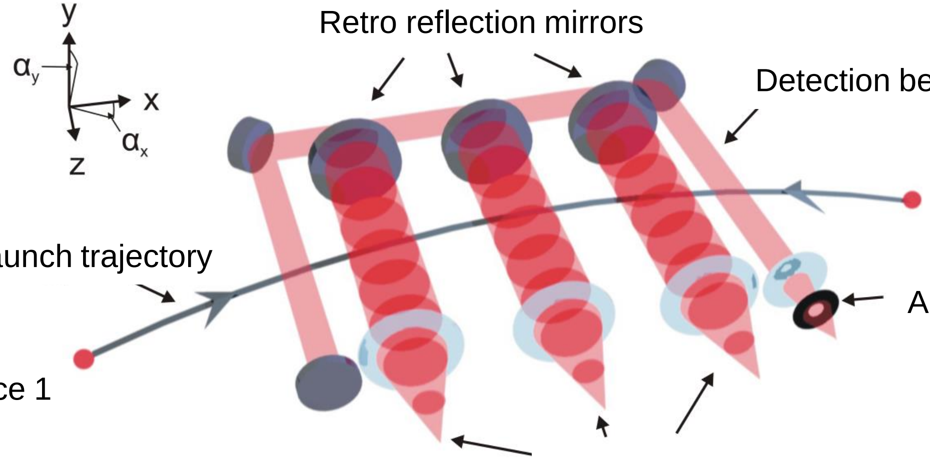

Image (modified) from [2]

<u>Double interferometer for measuring the rotation Ω_y:</u>

- 2 double MOT systems provide molasses cooled ^{87}Rb atoms at 10 µK
- Moving molasses launch to $v_{x,1} = 2.79\ \mathrm{m}/s$, $v_{x,2} = -2.79\ \mathrm{m}/s$; subsequent velocity filter
- 3 spatially separated interaction zones for Raman type beam splitters
- State-selective fluorescence detection detects 10^6 atoms per interferometer

[Images and results from: 1) Schubert, Dissertation, Leibniz Universität Hannover (2012); 2) Schubert, Dissertation, Leibniz Universität Hannover (2012), thanks to G. Tackmann for providing the image; see also: Berg at al., PRL 114, 063002 (2015); Tackmann et al., New J. Phys. 14, 015002, (2012)]

Discriminating rotations and accelerations

Signal of the two atom interferometers:

$$\phi_{1,2}(k_{1,2}, v_{x,1,2}) = 2(k_{1,2} \cdot v_{x,1,2}) \cdot \Omega_y \; T^2 + k_{1,2} \cdot a_z \; T^2 + \phi_{other,1,2}$$

$$k_1 = -k_2 = k, \; v_{x,1} = -v_{x,2} = v$$

Differential signal – acceleration:

$$\boldsymbol{\phi_{diff}} = [\phi_1 - (k, v)\phi_1(-k, -v)]/2 = \boldsymbol{k} \cdot \boldsymbol{a_z} \; \boldsymbol{T^2} + \phi_{other,diff}$$

Sum signal – rotation:

$$\boldsymbol{\phi_{sum}} = [\phi_1(k, v) + \phi_1(-k, -v)]/2 = \mathbf{2}(\boldsymbol{k} \cdot \boldsymbol{v}) \cdot \boldsymbol{\Omega_y} \; \boldsymbol{T^2} + \phi_{other,sum}$$

Symmetrized composite-pulse interferometer (SCI)

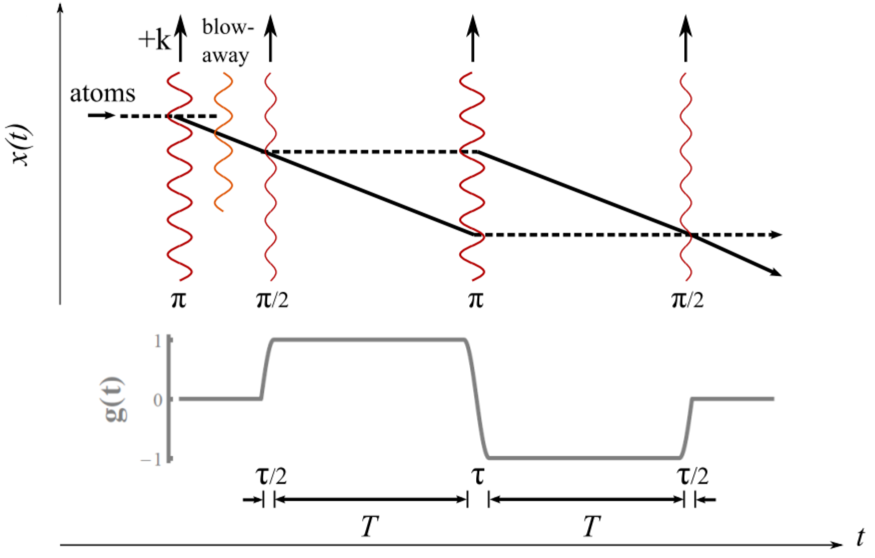

Image from [1]

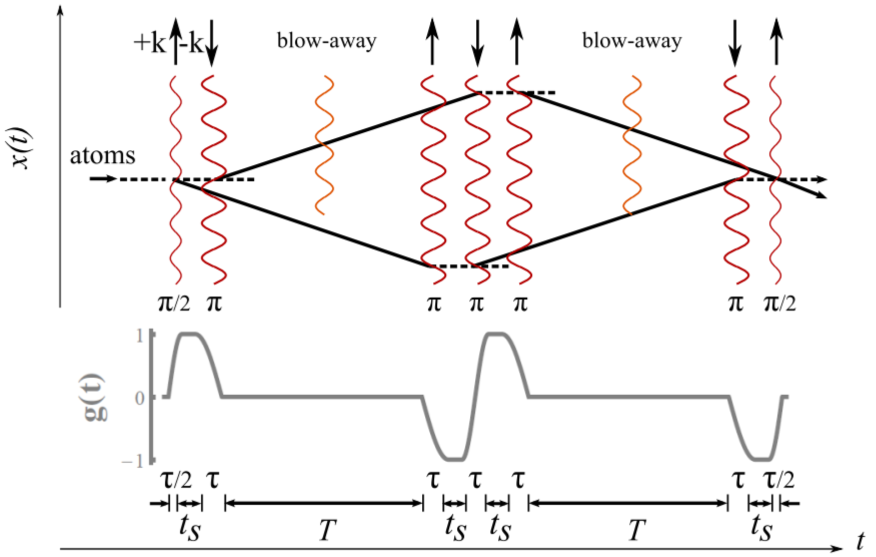

Image from [1]

MZI:

T_{MZI} = 24.7 ms, k_{MZI} = 4π/(780 nm), T_c = 0.5 s
C_{MZI} = 18 % (36 % at T_{MZI} = 23 ms)

Short-term instability MZI: **610 nrad/s** in **1 s**

SCI – larger k, noise suppression:

T_{SCI} = 25 ms, k_{SCI} = **8π/(780 nm)**, T_c = 0.5s
C_{SCI} = 19%

Short-term instability SCI: **120 rad/s** in **1 s**

[Images and results from: 1) Berg at al., PRL 114, 063002 (2015); 2) Tackmann et al., New J. Phys. 14, 015002, (2012)]

Results and limits of CASI in SCI configuration

DLR

Results:

- Short-term instability: **120 rad/s** in **1 s**
- Estimated intrinsic noise: 77 nrad/s in 1 s (detection, technical noise)
- Averaging: **26 rad/s** in **100 s** (higher background noise during operation, 260 rad/s in 1 s)
- Systematic uncertainty: **600 nrad/s** (uncertainty of launch velocity & starting position + wave front errors)

Possible improvements:

- Ultracold atoms / Bose-Einstein condensates (BECs) → improved contrast, reduced systematic error
- Lattice launch → improved control of launch vector / drift velocity
- Large momentum transfer → larger phase shift / improved sensitivity

[Results from: Berg at al., PRL 114, 063002 (2015)]

Rapid BEC generation on an atom chip

Atom-chip based BEC source for interferometry:

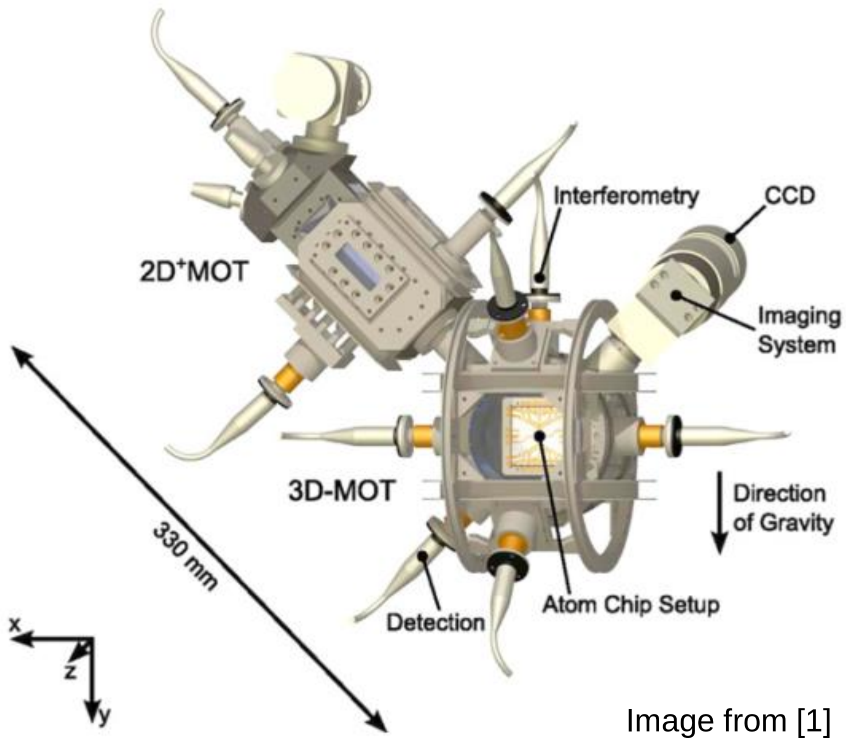

Image from [1]

Challenge:

- Providing high flux with low expansion rates of the atoms

Solution:

- Atom-chip based BEC generation + delta-kick collimation

Demonstrated flux [1]:

- $\{10^5, 4\cdot10^5\}$ ^{87}Rb atoms (BEC) in {1 s, 1.6 s}

Delta-kick collimation – lowering the velocity spread [2]:

- Down to a kinetic energy of $(3/2)k_B \cdot 38^{+6}_{-7}\,\mathrm{pK}$ (3D)

→ Reducing systematic errors, increasing short-term stability [3]

[Images and results from: 1) Rudolph et al., NJP 17, 065001 (2015), CC BY 3.0, https://creativecommons.org/licenses/by/3.0/; 2) Deppner et al., PRL 127, 100401 (2021); 3) Gebbe et al., Nat. Comm. 12, 2544 (2021); Szigeti et al., NJP 14, 023009 (2012); Louchet-Chauvet et al., NJP 13, 065025 (2011); Debs et al., Phys. Rev. A 84, 033610 (2011); Heine et al., EPJD 74, 174 (2020); Schkolnik et al., APB 120, 311 (2015); see also for rapid evaporation in optical dipole traps: Roy et al., arxiv:1601.05103; Albers et al., Comm. Phys. 5, 60 (2022)]

(Re)launching atoms

Retro-reflected beam setup – well-defined pointing of launch vector normal to mirror surface:

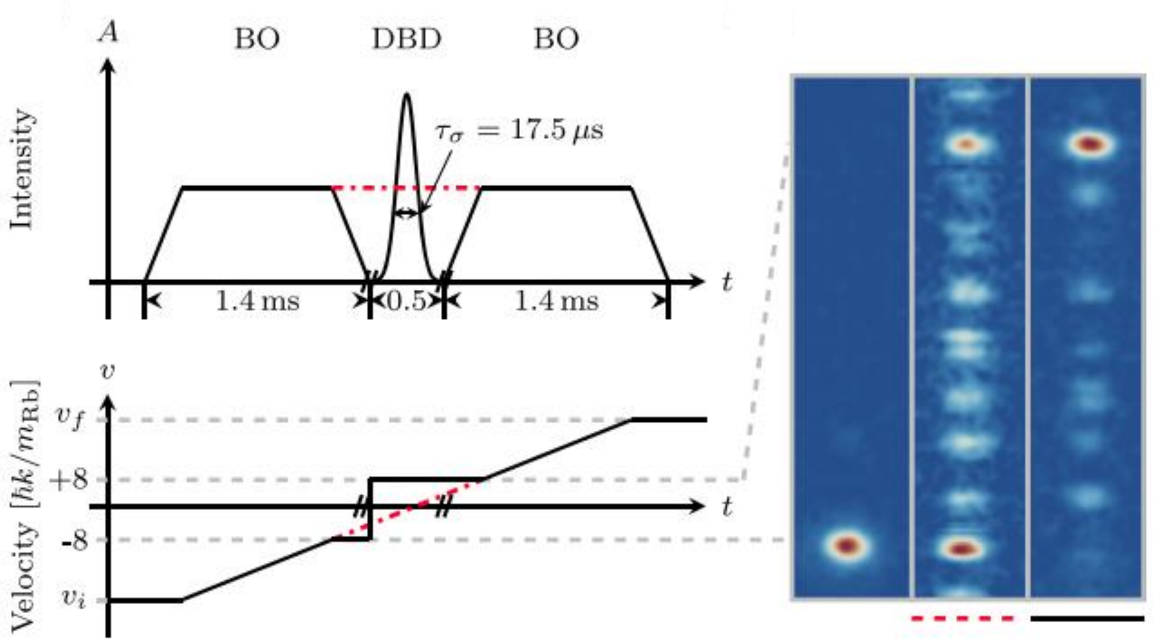

Image from [1]

<u>Challenge:</u>

- Losses due to simultaneous interaction with two moving lattices

<u>Solution [1]:</u>

- (De-)acceleration via Bloch oscillations (BO)
- 16 ħk double-Bragg pulse (DBD) inverts momentum around 0 momentum

<u>Demonstrated results [1]:</u>

- Launch efficiency of 75 % observed

→ Control of launch vector / drift velocity

[Images and results from: 1) Abend et al., PRL 117, 203003 (2016); see also: Dickerson et al., PRL 111, 083001 (2013)]

Large momentum transfer – twin lattice atom interferometer

Increasing the enclosed area / effectively k:

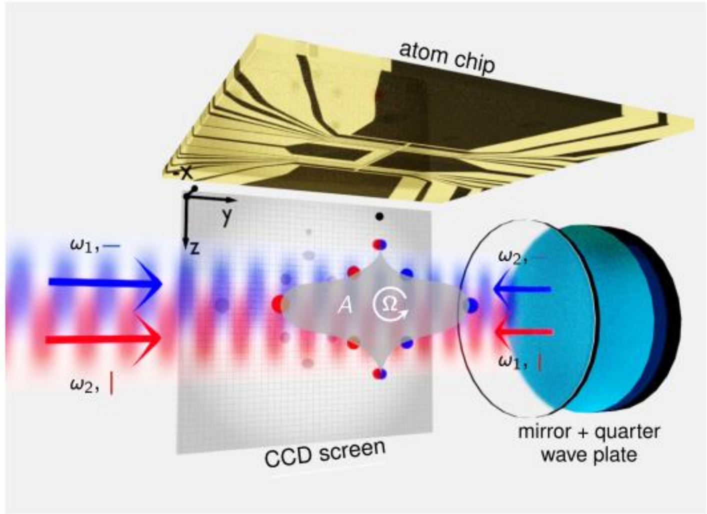

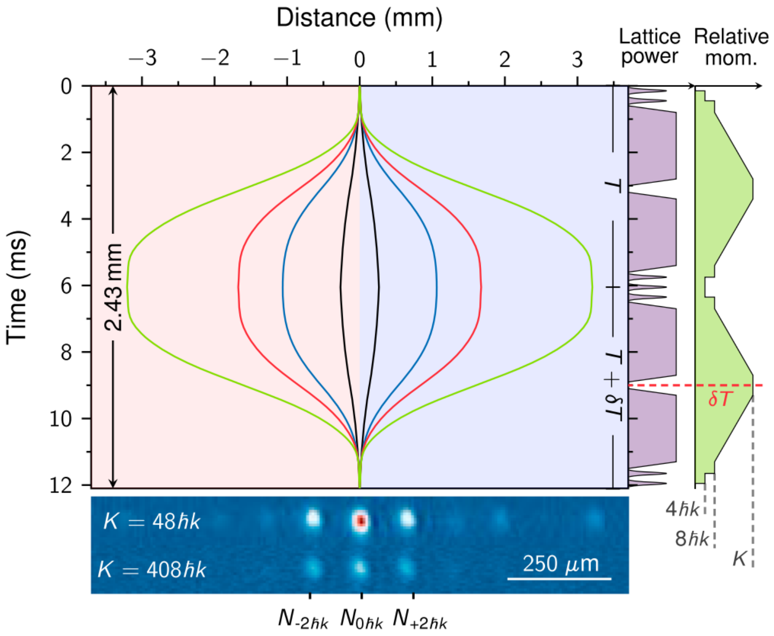

Challenge:

- Increasing k without losing contrast

Solution:

- Delta-kick collimated BEC
- Combining Bloch oscillations and double Bragg diffraction

Experimental results [1]:

- Realisation of interferometers with up to 408 ħk beam splitters
- Total transfer of up to 1632 ħk
- Remaining contrast: 14%

→ Increasing the scale factor for future interferometers

[Images and results from: 1) Gebbe et al., Nat. Comm. 12, 2544 (2021), CC BY 4.0; other LMTs: Lévèque et al., PRL 103, 080405 (2009); Müller et al., PRL 102, 240403 (2009); Chiow et al., PRL 107, 130403 (2011); Rudolph et al., PRL 124, 083604 (2020); ...]

Differential BEC interferometer

Demonstrating a double-interferometer scheme with a single BEC source:

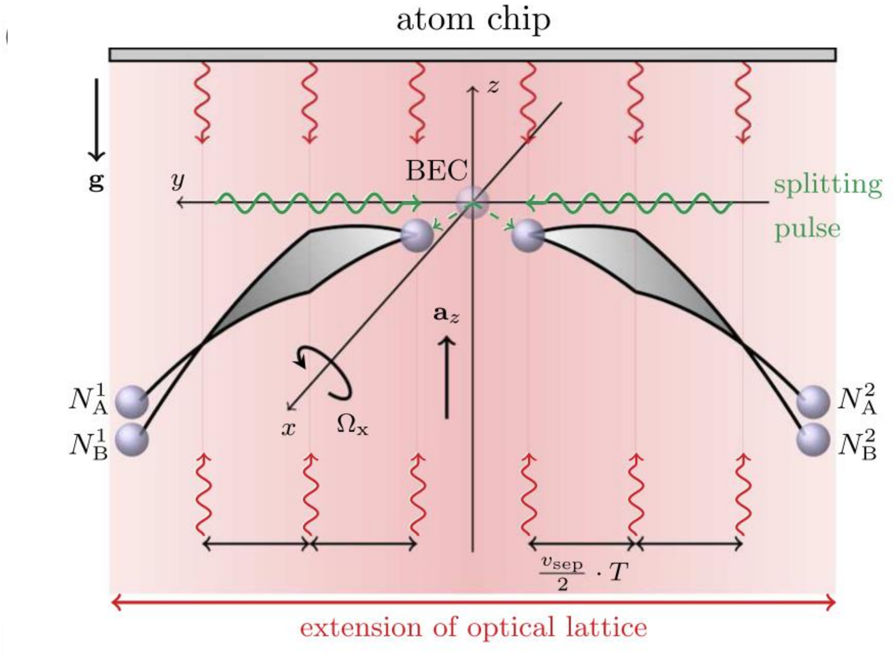

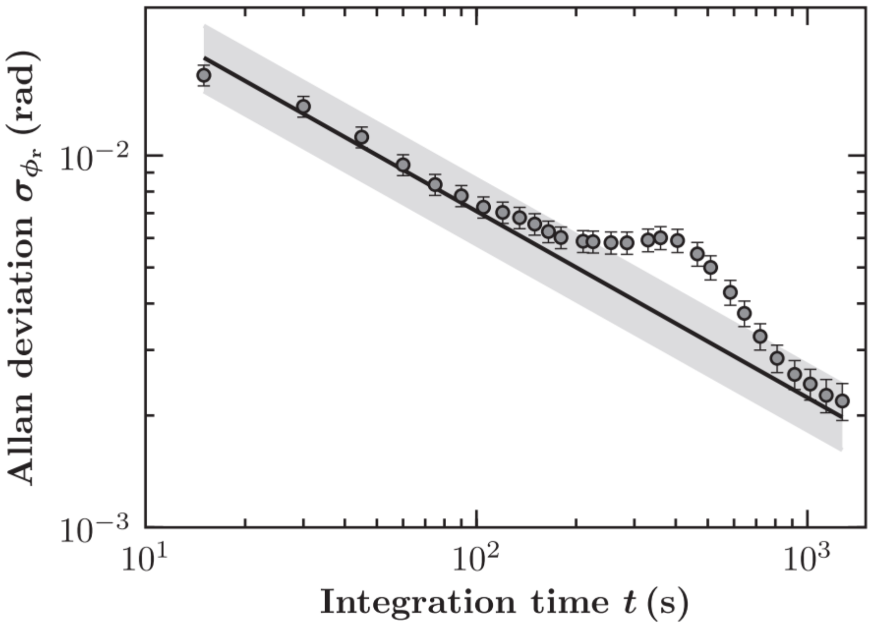

T = 5 ms, k = 4π/(780nm),
v = ħk/m ≈ 24 mm/s, T_c = 15 s

Short-term instability: **1.7 mrad/s** in **15 s**
(compatible with estimated shot noise limit)

[Images and results from: 1) Gersemann et al., EPJD 74, 203 (2020), CC BY 4.0]

Novel multi-loop scheme – motivation

Stable, absolute rotation measurement with freely falling atoms

- Multiple round trips of the atoms → linear increase in effectively enclosed area similar to fibre optical gyroscopes [1] → boosted sensitivity without increasing the size of the vacuum vessel / sensor head [2]

- Multi-loop scheme based on symmetric beam splitting and relaunches [2]

- Anticipated sensitivity: $2 \cdot 10^{-11}\ \mathrm{rad}/s$ in 1 s [2], comparable to the large ring laser gyroscope in Wettzell [3]

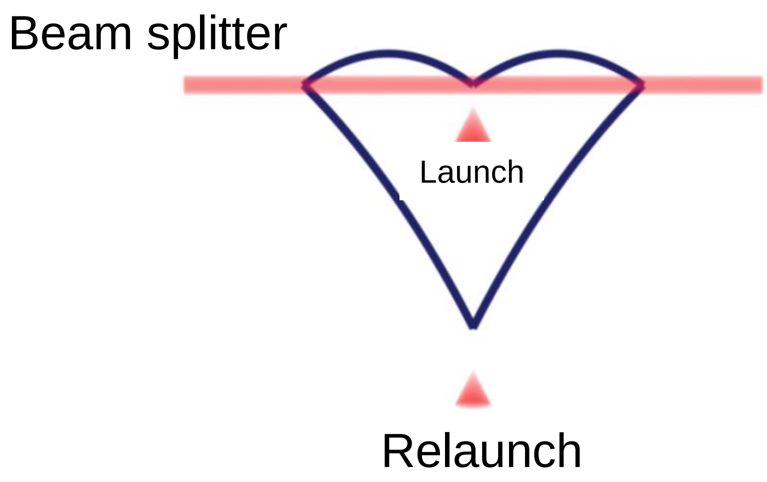

[1) Jekeli, Navigation 52, 1–14 (2005); 2) Schubert et al., Sci. Rep. 11, 16121 (2021), CC BY 4.0; 3) Gebauer et al., PRL 125, 033605 (2020)]

Previously published results & features of novel multi-loop scheme

Previous implementations [1-3]:

- Based on 3-pulse, Mach-Zehnder-like or 4-pulse, ‘butterfly’ geometries
- Thermal Cs beam, molasses cooled Cs / Rb injected into the interferometer
- Tuneability of pulse-separation time typically limited by optical access / spatially separated beam splitters
- Spatially separated atom-light-interaction zones require fine adjustment

Features of proposed scheme [4]:

- Tunable free-fall time → scalable area
- Coherent atom-light interactions imprint velocities → well-defined area
- Beam splitting on single axis → no relative alignment required
- Symmetric beam splitting → reduced biases due to light shifts
- Multiple beam splitting axes → compatible with measurements of tilt, gravity

[1) Durfee et al., PRL 97, 240801 (2006); 2) Gauguet et al., PRA 80, 063604 (2009); Stockton et al., PRL 107, 133001 (2011); Berg et al., PRL 114, 063002 (2015); 3) Savoie et al. Sci. Adv. 4, eaau7948 (2018); Gautier et al., Sci. Adv. 8, eabn8009 (2022); 4) Schubert et al., Sci. Rep. 11, 16121 (2021), CC BY 4.0]

Implementation of the multi-loop geometry

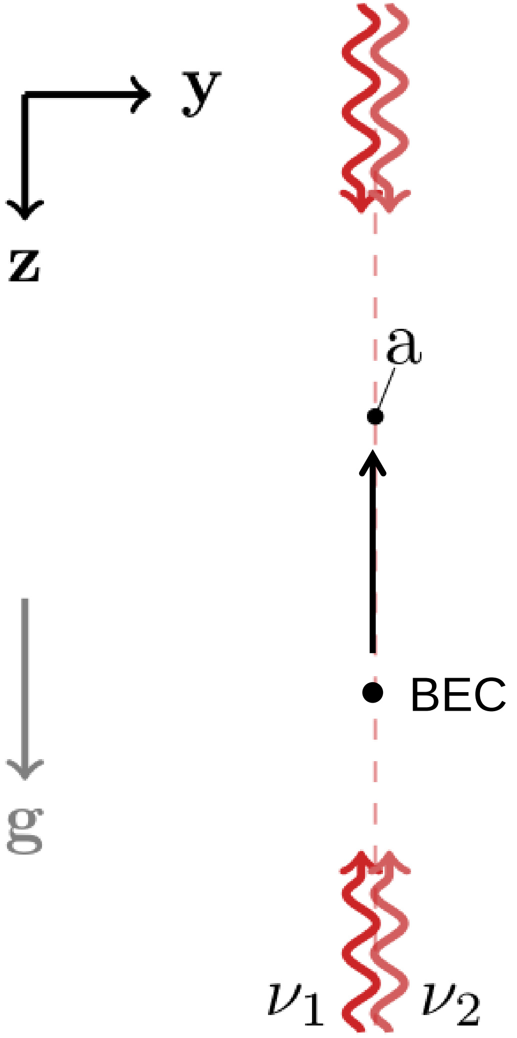

- Launch BEC (small initial momentum & low expansion rate)

[Schubert et al., Sci. Rep. 11, 16121 (2021); slide (modified) from M. Gersemann, LUH]

Implementation of the multi-loop geometry

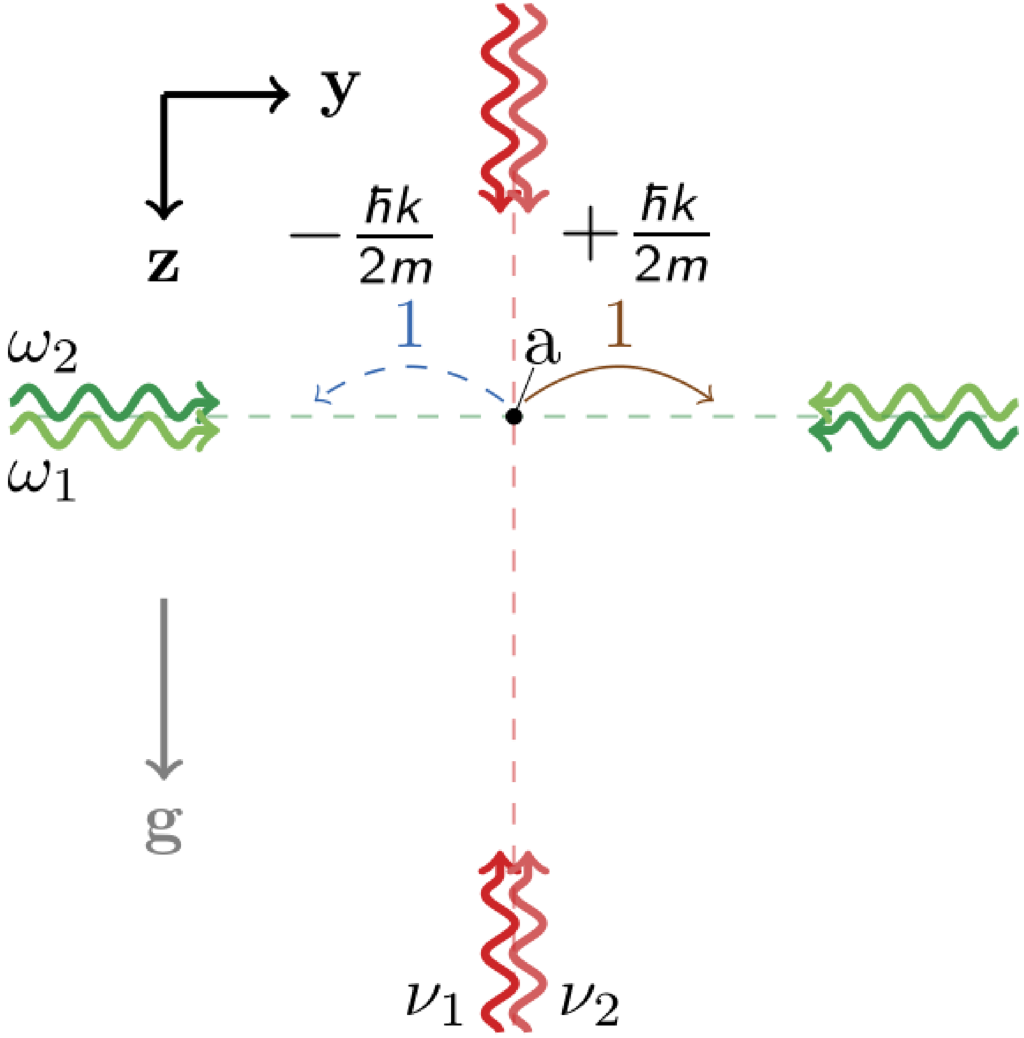

- Launch BEC (small initial momentum & low expansion rate)
- Horizontal beam splitter: two wave packets drifting apart (a)

[Schubert et al., Sci. Rep. 11, 16121 (2021); slide (modified) from M. Gersemann, LUH]

Implementation of the multi-loop geometry

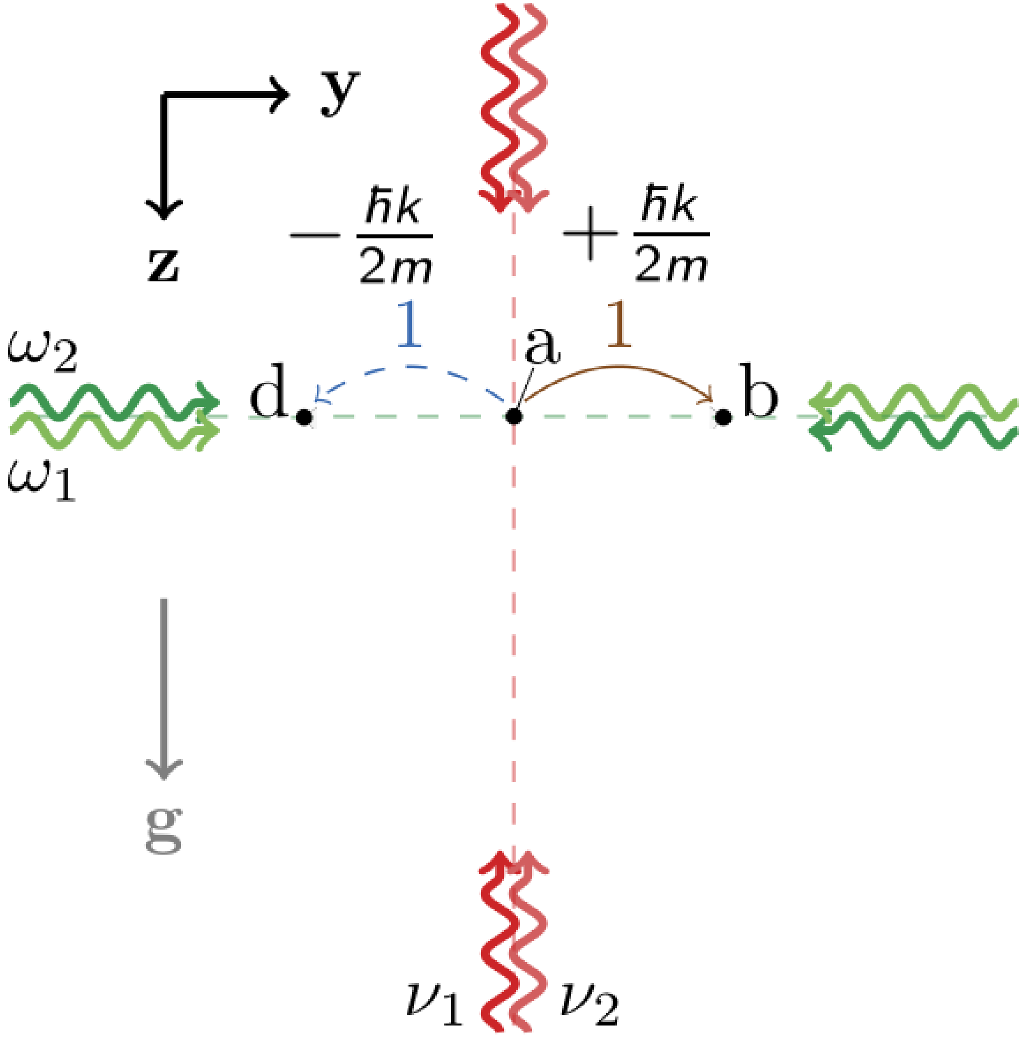

- Launch BEC (small initial momentum & low expansion rate)
- Horizontal beam splitter: two wave packets drifting apart (a)
- After time *T*, invert the movement of the atoms (b,d)

[Schubert et al., Sci. Rep. 11, 16121 (2021); slide (modified) from M. Gersemann, LUH]

Implementation of the multi-loop geometry

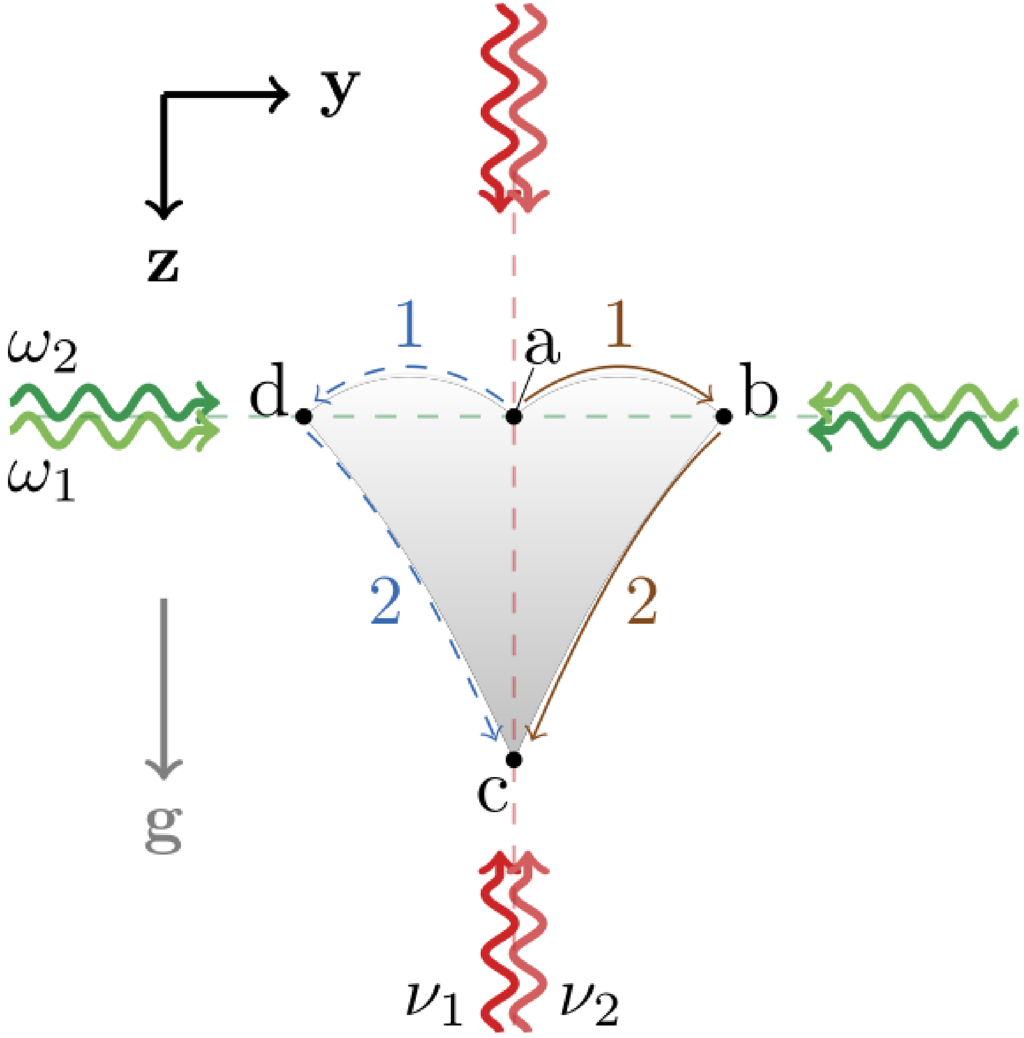

- Launch BEC (small initial momentum & low expansion rate)
- Horizontal beam splitter: two wave packets drifting apart (a)
- After time *T*, invert the movement of the atoms (b,d)
- After time 2*T*, relaunch atoms and revert momentum (c)

[Schubert et al., Sci. Rep. 11, 16121 (2021); slide (modified) from M. Gersemann, LUH]

Implementation of the multi-loop geometry

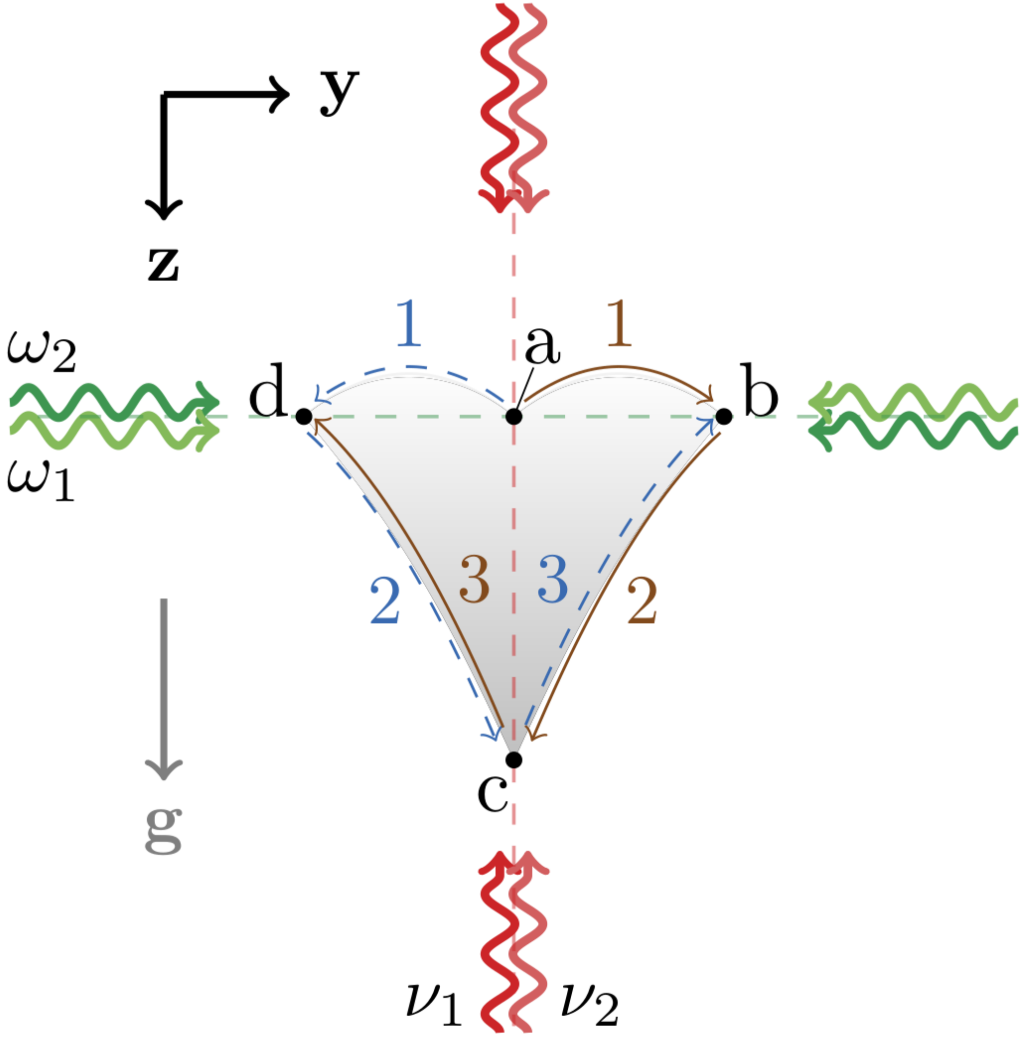

- Launch BEC (small initial momentum & low expansion rate)
- Horizontal beam splitter: two wave packets drifting apart (a)
- After time *T*, invert the movement of the atoms (b,d)
- After time 2*T*, relaunch atoms and revert momentum (c)
- After time 3*T*, deflect atoms towards each other (b,d)

[Schubert et al., Sci. Rep. 11, 16121 (2021); slide (modified) from M. Gersemann, LUH]

Implementation of the multi-loop geometry

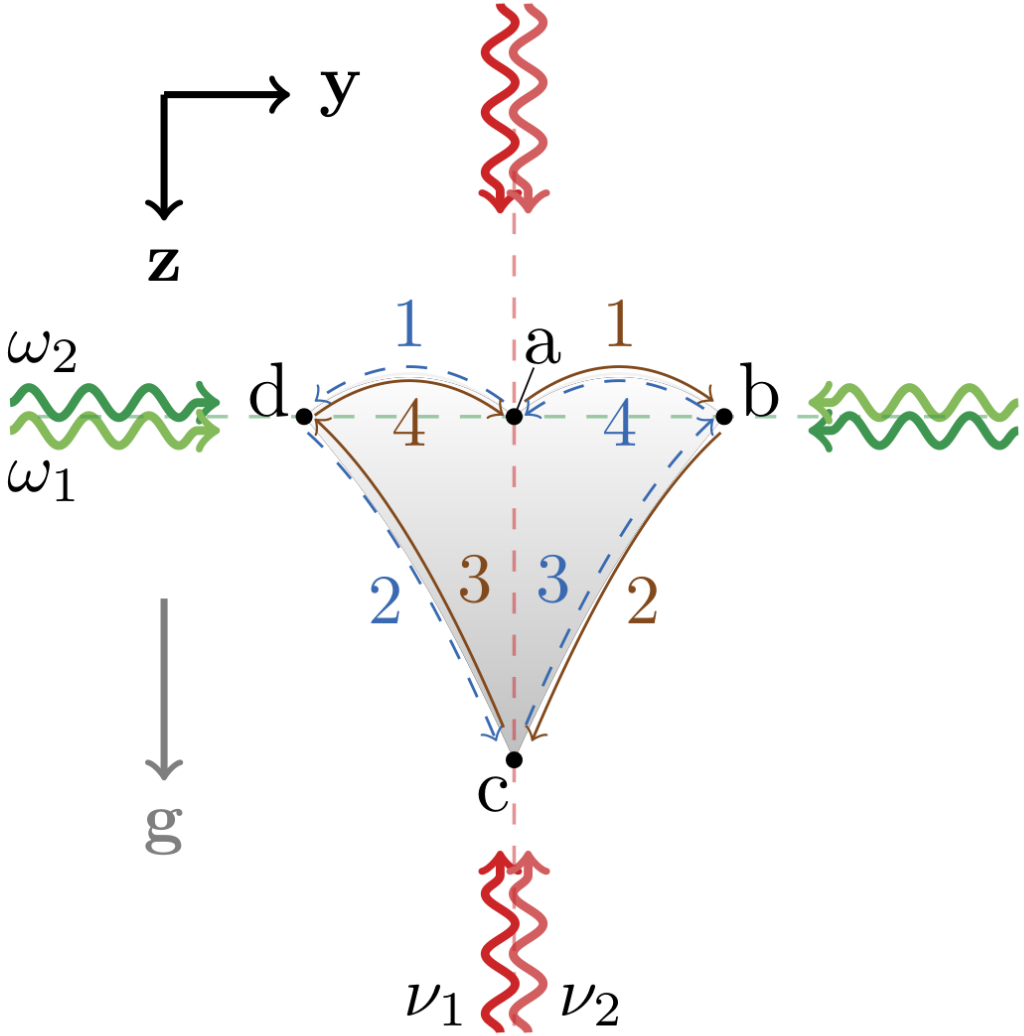

- Launch BEC (small initial momentum & low expansion rate)
- Horizontal beam splitter: two wave packets drifting apart (a)
- After time *T*, invert the movement of the atoms (b,d)
- After time 2*T*, relaunch atoms and revert momentum (c)
- After time 3*T*, deflect atoms towards each other (b,d)
- After time *4T*, atoms cross falling downwards (a)

[Schubert et al., Sci. Rep. 11, 16121 (2021); slide (modified) from M. Gersemann, LUH]

Implementation of the multi-loop geometry

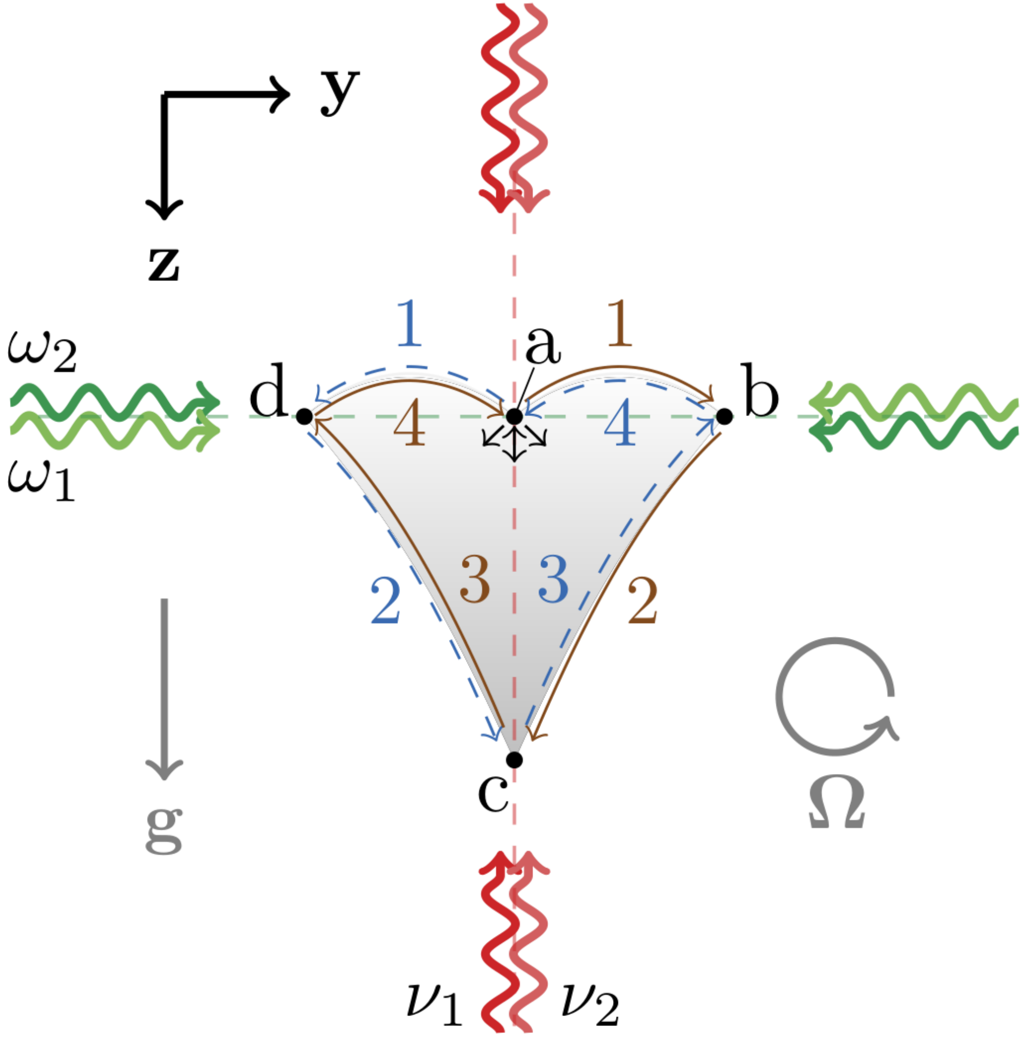

- Launch BEC (small initial momentum & low expansion rate)
- Horizontal beam splitter: two wave packets drifting apart (a)
- After time *T*, invert the movement of the atoms (b,d)
- After time 2*T*, relaunch atoms and revert momentum (c)
- After time 3*T*, deflect atoms towards each other (b,d)
- After time *4T*, atoms cross falling downwards (a)

Two options:

1. Repeat sequence → form another 2*n* loop
2. Close interferometer and read out phase

[Schubert et al., Sci. Rep. 11, 16121 (2021); slide (modified) from M. Gersemann, LUH]

Multi-loop geometry

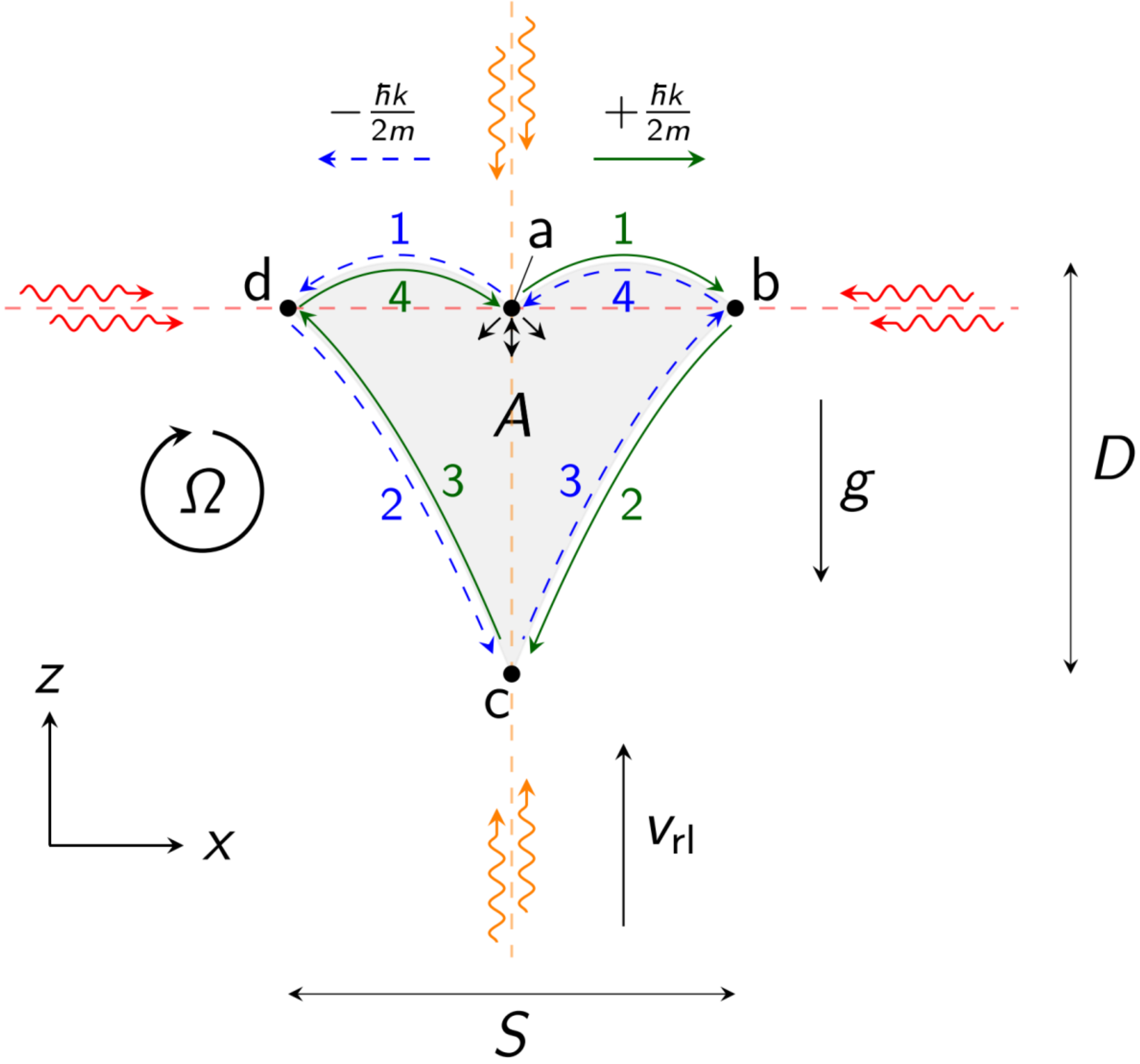

Single (~butterfly / double loop) or multiple round trips

Relaunch velocity: $v_{rl} = |\boldsymbol{v}_{rl}| = 3gT$

Enclosed area: $A = n \cdot 2\frac{\hbar k}{m} gT^3$

Phase shift: $\Delta\phi_{Sagnac} = n \cdot (\boldsymbol{k} \times \boldsymbol{g})\boldsymbol{\Omega} T^3$

Wavevector $\boldsymbol{k}$, gravitational acceleration $\boldsymbol{g}$, rotation $\boldsymbol{\Omega}$, atomic mass m, number of round trips n

[Image and results from: 2) Schubert et al., Sci. Rep. 11, 16121 (2021), CC BY 4.0]

Pulse timings

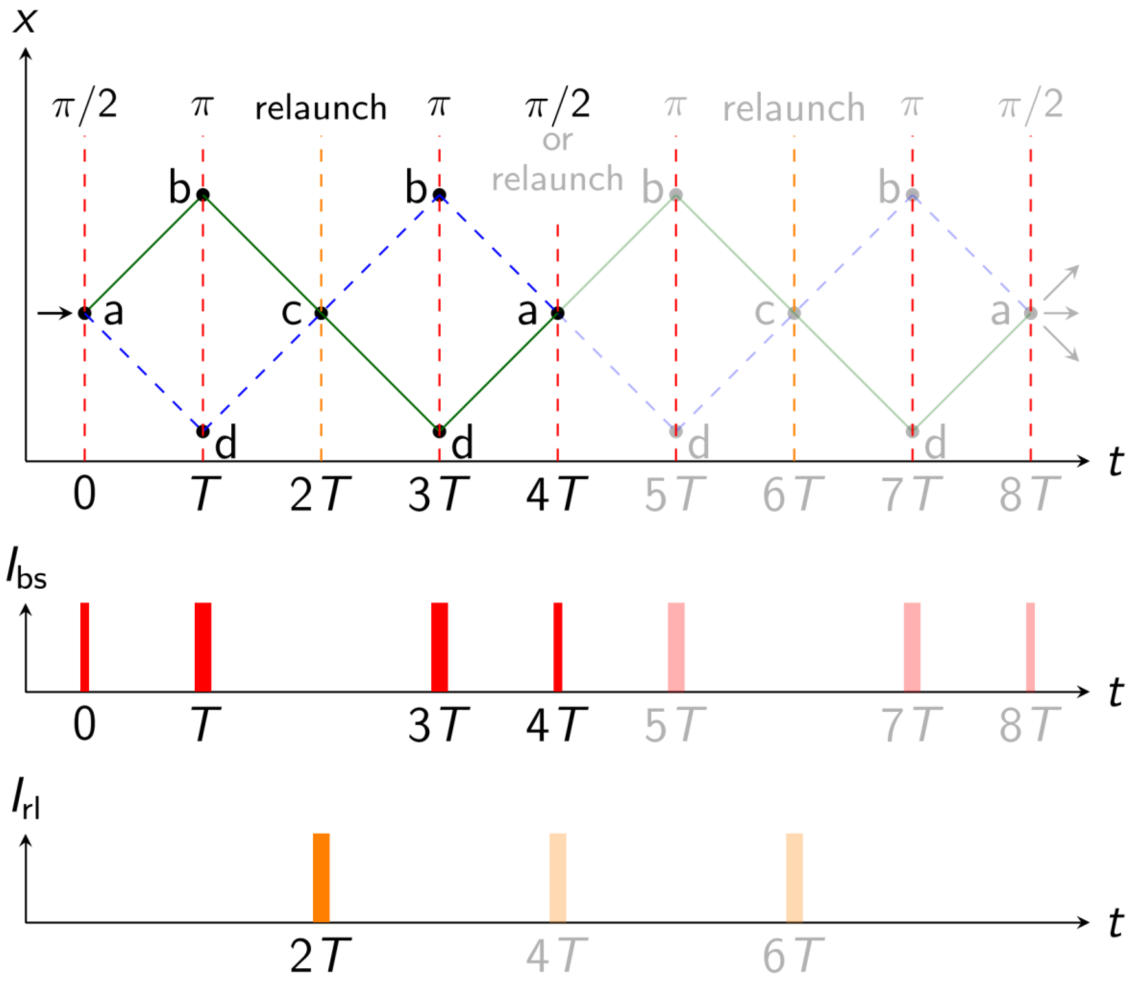

Single round trip – 2 loops:

- 4 beam splitting pulses: $\pi/2 - \pi - \pi - \pi/2$
- Pulse separation: T – 2T – T
- Relaunch at 2T
- Recombination at 4T

Extension to multi-loop operation by relaunch instead of recombination

Beam splitter intensity I_{bs}, relaunch pulse intensity I_{rl} (not to scale)

[Image and results from: Schubert et al., Sci. Rep. 11, 16121 (2021), CC BY 4.0]

Anticipated sensitivities

Sensor features	N	$k\left(\frac{2\pi}{780\,\text{nm}}\right)$	T (ms)	n	C	A (m^2)	t_c (s)	S (m)	D (m)	Sensitivity $\left(\frac{\text{rad/s}}{\sqrt{\text{Hz}}}\right)$
1: Multi loop	10^5	**40**	10	10	1	4.6×10^{-5}	1.6	$\mathbf{2.4 \times 10^{-3}}$	$\mathbf{2.8 \times 10^{-3}}$	3.2×10^{-8}
1: Four pulse	10^5	**350**	10	–	1	4×10^{-5}	1.24	$\mathbf{2.1 \times 10^{-2}}$	$\mathbf{5 \times 10^{-3}}$	3.2×10^{-8}
2: Multi loop	4×10^5	20	250	10	1	$\mathbf{3.6 \times 10^{-1}}$	**11.8**	3×10^{-2}	0.7	$\mathbf{5.5 \times 10^{-12}}$
2: Four pulse	4×10^5	28	189	–	1	$\mathbf{2.1 \times 10^{-2}}$	**2.8**	3.1×10^{-2}	0.7	$\mathbf{4.2 \times 10^{-11}}$
Compact	5.9×10^4	40	10	6	0.53	2.8×10^{-5}	1.44	2.4×10^{-3}	2.8×10^{-3}	1.2×10^{-7}
High sensitivity	2.9×10^5	20	250	4	0.66	1.4×10^{-1}	5.8	3×10^{-2}	0.7	1.7×10^{-11}

Drop distance: $D = (3T/2)^2 \cdot g/2$

Maximum trajectory separation: $S = \hbar kT/m$

Quantum projection noise limit: $\sigma_\Omega(t) = \frac{1}{C\sqrt{N}\cdot n\cdot(4kgT^3)}\sqrt{\frac{t_{prep}+n\cdot 4T+t_{det}}{t}}$

Double-loop dependent contrast: $C(n) = C(1)^n$

Loss factor: l^{n-1} with $l = 0.9$ for $2n$ loops

Contrast C, number of atoms N (modified by losses), averaging time t, preparation time t_{prep}, detection time t_{det}

[Table and results from: Schubert et al., Sci. Rep. 11, 16121 (2021), CC BY 4.0]

Error terms due to relaunch and other couplings

	$\alpha_{\delta\tau}$ (*rad*)	α_Γ	β	v_{x0} (μm/s)	v_{y0}	v_{z0}	y_0 (μm)	z_0	δg (m/s^2)	$\delta\Gamma$ (1/s^2)
Compact	1.3×10^{-4}	< 0.1	9.4×10^{-5}	200 *	250 †	250 †	100 ‡	100 ‡	5.6×10^{-4}	7.2×10^{-2}
High sensitivity	6×10^{-6}	2.5×10^{-6}	6.6×10^{-9}	26 ⋆	10 †	10 †	100 ‡	100 ‡	5.4×10^{-8}	1.1×10^{-8}

Assumptions:

- Phase errors $10n$ times below the quantum projection noise limit ($\sim 1/\sqrt{N}$); †velocity acceptance; ‡position w.r.t. beam
- $\Gamma_x = \Gamma_y = 0.5\Gamma_z = 1.5 \cdot 10^{-6}\ \mathrm{s}^{-2}$, $\Omega_x = \Omega_y = \Omega_z = 7.27 \cdot 10^{-5}\ \mathrm{rad/s}$, *gradient compensation to 0.1Γ

Error terms due to imperfect pointing of the relaunch vector $\boldsymbol{v}_{rl}$:

- Relaunch tilt α and timing error $\delta\tau$: $\Delta\phi_{\alpha,\tau} = -kv_{rl}\alpha\delta\tau = -3kgT\alpha\delta\tau$
- Relaunch tilt α and gravity gradient Γ: $\Delta\phi_{\alpha,\Gamma} = \boldsymbol{k}\Gamma\boldsymbol{v}_{rl}T^3 = 3k\alpha\Gamma_x gT^4$
- Relaunch tilt β and rotation Ω: $\Delta\phi_{\beta,\Omega} = 2(\boldsymbol{k} \times \boldsymbol{v}_{rl})\boldsymbol{\Omega}\mathbf{T}^2 = 6k\beta g\Omega_z T^3$

Dominant error terms depending on starting position (x_0, y_0, z_0) / velocity $\boldsymbol{v}$ and others:

- Velocity v_x: $\Delta\phi_{vx} = 4kT^3\left(\Gamma_x + 3\left(\Omega_y^2 + \Omega_z^2\right)\right)v_x$
- Velocity v_y: $\Delta\phi_{vy} = -4kT^3\left(3\Omega_x\Omega_y + 4T\left(\Gamma_x + \Gamma_y\right)\Omega_z\right)v_y$
- Velocity v_z: $\Delta\phi_{vz} = -4kT^3\left(3\Omega_x\Omega_z + 4T(\Gamma_z + \Gamma_x)\Omega_y\right)v_z$
- Position y_0: $\Delta\phi_{y0} = 8kT^3\Gamma_y\Omega_z y_0$
- Position z_0: $\Delta\phi_{z0} = -8kT^3\Gamma_z\Omega_y z_0$
- Others: $\Delta\phi_{\Gamma x} = 18kT^5\Omega_y\Gamma_x$, $\Delta\phi_{\Gamma z} = 18kT^5\Omega_y\Gamma_z$

[Table and results from: Schubert et al., Sci. Rep. 11, 16121 (2021), CC BY 4.0]

Perspectives

Multi-loop rotation sensor:

- Compact sensor: $1.2 \cdot 10^{-7}\ (\mathrm{rad/s})/\sqrt{\mathrm{Hz}}$ within a volume of 20 mm^3
- Highly sensitive setup: $1.7 \cdot 10^{-11}\ (\mathrm{rad/s})/\sqrt{\mathrm{Hz}}$ within a meter-sized vacuum vessel
- Compatible with implementing tilt & gravity measurements in the same setup
- Detection of multiple rotation axes by adding perpendicular horizontal beam splitter

[Schubert et al., Sci. Rep. 11, 16121 (2021), CC BY 4.0]

Summary & conclusion

Features & status:

- Atom interferometry: a tool for absolute, long-term stable rotation (and acceleration) measurements
- Demonstrated instability: 30 nrad/s in 1 s, 0.1 nrad/s after averaging
- Systematic uncertainty: few 100 nrad/s; systematic error limited by wave front distortions

Pathways for improvement:

- Ultracold atoms / BEC + DKC
- Lattice (re)launch
- Large momentum transfer (e.g. twin-lattice atom interferometer)
- Multi-loop schemes – up to $1.7 \cdot 10^{-11}\ (\mathrm{rad/s})/\sqrt{\mathrm{Hz}}$ within a meter-sized vacuum vessel

THANK YOU

Christian.Schubert@dlr.de

DLR

Summary & conclusion

Features & status:

- Atom interferometry: a tool for absolute, long-term stable rotation (and acceleration) measurements
- Demonstrated instability: 30 nrad/s in 1 s, 0.1 nrad/s after averaging
- Systematic uncertainty: few 100 nrad/s; systematic error limited by wave front distortions

Pathways for improvement:

- Ultracold atoms / BEC + DKC
- Lattice (re)launch
- Large momentum transfer (e.g. twin-lattice atom interferometer)
- Multi-loop schemes – up to $1.7 \cdot 10^{-11}\ (\mathrm{rad/s})/\sqrt{\mathrm{Hz}}$ within a meter-sized vacuum vessel

See poster by M. Gersemann

Positions available!